This article was downloaded by:
On: *30 January 2011*
Access details: *Access Details: Free Access*
Publisher *Taylor & Francis*
Informa Ltd Registered in England and Wales Registered Number: 1072954 Registered office: Mortimer House, 37-41 Mortimer Street, London W1T 3JH, UK

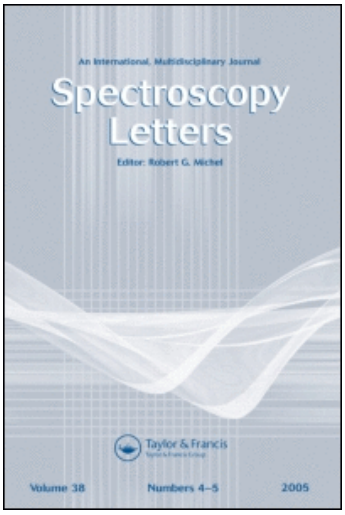

Spectroscopy Letters
Publication details, including instructions for authors and subscription information:
http://www.informaworld.com/smpp/title~content=t713597299

Wavelength-Dependent Photolysis of C3-C7 Aldehydes in the 280-330 nm Region

Lei Zhu[ab]; Yongxin Tang[ab]; Yunqing Chen[ab]; Thomas Cronin[ab]
[a] Wadsworth Center, New York State Department of Health, Albany, New York, USA [b] Department of Environmental Health Sciences, State University of New York, Albany, New York, USA

Online publication date: 01 December 2009

To cite this Article Zhu, Lei , Tang, Yongxin , Chen, Yunqing and Cronin, Thomas(2009) 'Wavelength-Dependent Photolysis of C3-C7 Aldehydes in the 280-330 nm Region', Spectroscopy Letters, 42: 8, 467 — 478
To link to this Article: DOI: 10.1080/00387010903267195
URL: http://dx.doi.org/10.1080/00387010903267195

PLEASE SCROLL DOWN FOR ARTICLE

Full terms and conditions of use: http://www.informaworld.com/terms-and-conditions-of-access.pdf

This article may be used for research, teaching and private study purposes. Any substantial or systematic reproduction, re-distribution, re-selling, loan or sub-licensing, systematic supply or distribution in any form to anyone is expressly forbidden.

The publisher does not give any warranty express or implied or make any representation that the contents will be complete or accurate or up to date. The accuracy of any instructions, formulae and drug doses should be independently verified with primary sources. The publisher shall not be liable for any loss, actions, claims, proceedings, demand or costs or damages whatsoever or howsoever caused arising directly or indirectly in connection with or arising out of the use of this material.

Spectroscopy Letters, 42:467–478, 2009
Copyright © Taylor & Francis Group, LLC
ISSN: 0038-7010 print/1532-2289 online
DOI: 10.1080/00387010903267195

Taylor & Francis
Taylor & Francis Group

Wavelength-Dependent Photolysis of C3-C7 Aldehydes in the 280–330 nm Region

**Lei Zhu,
Yongxin Tang,
Yunqing Chen,
and Thomas Cronin**

Wadsworth Center, New York State Department of Health, and Department of Environmental Health Sciences, State University of New York, Albany, New York, USA

Downloaded At: 02:46 30 January 2011

ABSTRACT This article reviews the work over the past few years on the photolysis of propionaldehyde, n-butyraldehyde, n-pentanal, n-hexanal, and n-heptanal in the 280–330 nm region, obtained by combining laser photolysis with cavity ring-down spectroscopy. Absorption cross-sections of these aldehydes were measured. The HCO radical was observed as a photodissociation product. The HCO quantum yield was determined as a function of photolysis wavelength, aldehyde pressure, and nitrogen buffer-gas pressure. A scheme to group aldehydes according to similarity in photochemistry was proposed.

KEYWORDS absorption cross sections, aldehydes, cavity ring-down spectroscopy, photodissociation rate and lifetime, photolysis, radical quantum yields

INTRODUCTION

Aliphatic aldehydes are introduced into the atmosphere through biogenic and anthropogenic emissions and through photo-oxidation of tropospheric organic compounds. Their atmospheric chemistry has been studied extensively as a result of their central role in the formation of photochemical smog, peroxyacetyl nitrate (PAN), and ground-level ozone.[1,2] The major gas-phase removal pathways for saturated aliphatic aldehydes in the atmosphere are reactions with OH radicals and unimolecular photodissociation. Rate constants for OH radical reactions with C_1-C_7 aldehydes have been reported previously.[3–11] Photodissociation of aldehydes is an important source of free radicals in the atmosphere.[12] The photolysis of formaldehyde (CH_2O) and acetaldehyde (CH_3CHO) has been studied extensively.[13–16] Determination of the wavelength-dependent photolysis quantum yields of propionaldehyde (C_2H_5CHO), n-butyraldehyde ($CH_3(CH_2)_2CHO$), n-pentanal ($CH_3(CH_2)_3CHO$), n-hexanal ($CH_3(CH_2)_4CHO$), and n-heptanal ($CH_3(CH_2)_5CHO$) is necessary to elucidate their atmospheric photodissociation fates and to establish the relationship between product quantum yields and aldehyde alkyl chain length. Such a determination also permits an estimation of the aldehyde tropospheric radical formation rates.

Aliphatic aldehydes exhibit a weak UV absorption band in the 240–360 nm region as a result of an electric dipole-forbidden but vibronically allowed $n \rightarrow *$ transition.[17] The thermodynamically allowed dissociation pathways,

Received 6 November 2006; accepted 28 March 2007.

Address correspondence to Lei Zhu, Wadsworth Center, New York State Department of Health, Empire State Plaza, P.O. Box 509, Albany, NY 12201-0509. E-mail: zhul@wadsworth.org

following excitation in the UV region, are as follows:

$$\mathrm{RCHO} + h\nu \longrightarrow \mathrm{R} + \mathrm{HCO}\ (\lambda \leq 339\ \mathrm{nm}), \quad (1)$$

$$\longrightarrow \mathrm{RH} + \mathrm{CO}\ (\mathrm{all}\ \lambda), \quad (2)$$

$$\longrightarrow \mathrm{R'H} + [\mathrm{CH_2{=}CHOH}] \longleftrightarrow \mathrm{R'H} + \mathrm{CH_3CHO}$$
$$(\lambda \leq 978\ \mathrm{nm\ for\ R'} = \mathrm{C_2H_3}, \mathrm{C_3H_5}, \mathrm{C_4H_7}, \mathrm{C_5H_9}), \quad (3)$$

$$\longrightarrow \mathrm{RCO} + \mathrm{H}\ (\lambda \leq 306\ \mathrm{nm}), \quad (4)$$

$$\longrightarrow \text{2-methyl-cyclo-R''} - \mathrm{OH}$$
$$(\lambda \leq 1300\ \mathrm{nm\ for\ R''} = \mathrm{C_5H_8}\ \mathrm{and}\ \mathrm{C_6H_{10}}), \quad (5)$$

$$\longrightarrow \text{2-ethyl-cyclo-R}^{\mathrm{III}} - \mathrm{OH}$$
$$(\lambda \leq 1300\ \mathrm{nm\ for\ R^{III}} = \mathrm{C_4H_6}\ \mathrm{and}\ \mathrm{C_5H_8}), \quad (6)$$

where threshold wavelengths were calculated from the corresponding enthalpy changes. Photolysis channels 1, 2, and 3 are radical formation, molecular elimination, and Norrish II channels, respectively. Channel 4, another radical-formation channel, was found to be minor for aliphatic aldehydes.[18] Channels 5 and 6 are photocyclization channels; they are available for >Cs aldehydes.

In this article, previous work is reviewed on the photolysis of propionaldehyde,[19] n-butyraldehyde,[20] n-pentanal,[21] n-hexanal,[22] and n-heptanal,[22] determined at 5-nm intervals in the 280–330 nm region with results obtained using dye laser photolysis combined with cavity ring-down spectroscopy.[23,24] Absorption cross-sections for the aldehydes have been determined over the wavelength range of 280–330 nm. The HCO quantum yield from the photolysis of these aldehydes, and its dependence on photolysis wavelength, aldehyde pressure, and nitrogen buffer-gas pressure, have been determined. The absolute HCO radical concentration was calibrated either relative to formaldehyde photolysis, $\mathrm{HCHO}+h\nu \rightarrow \mathrm{H}+\mathrm{HCO}$, for which the recommended HCO radical yield at each photolysis wavelength is available,[25] or relative to the $\mathrm{Cl}+\mathrm{CH_2O} \rightarrow \mathrm{HCl}+\mathrm{HCO}$ reaction.[25] Radical formation rates from the photolysis of C3-C7 aldehydes have been estimated as a function of zenith angle for cloudless conditions at sea level and at 760 Torr nitrogen pressure. Assuming a photolysis quantum yield of unity for C3-C7 aldehydes in the actinic UV region, the atmospheric photodissociation lifetimes of these aldehydes are also reported.

EXPERIMENTAL

The experimental setup has been described in detail elsewhere.[21,26–28] Two laser systems were used in the experiments. One laser was used to photolyze the aldehydes, and the other was used to probe the HCO radical. The second-harmonic output of a tunable dye laser pumped by a 308 nm XeCl excimer laser (~200 mJ/pulse) was used as photolysis radiation. Laser dyes used were coumarin 153, rhodamine 6 G, rhodamine B, rhodamine 101, sulforhodamine 101, and 4-dicyanmethylene-2-methyl-6-p-dimethylaminostyryl-4H-pyran (DCM). The photolysis laser beam entered the reaction cell through a sidearm at a 15-degree angle to the main cell axis. The probe laser beam (613–617 nm; 0.01-nm laser bandwidth) from a nitrogen-pumped dye laser was directed along the main optical axis of the cell. The pump and the probe laser beams overlapped one another at the center of the reaction cell, which was vacuum-sealed with a pair of high-reflectance cavity mirrors. The base path length between the two cavity mirrors was 50 cm. A fraction of the probe laser pulse was injected into the cavity through the front mirror, and its intensity decayed as the light bounced back and forth inside the cell. The light-intensity decay inside the cavity was measured by monitoring the weak transmission of light through the rear mirror with a photomultiplier tube (PMT). The PMT output was amplified, digitized, and sent to a computer. The decay curve was fitted to a single-exponential decay function. The ring-down time constant and the total loss per optical pass were calculated. By measuring the cavity losses with and without a photolysis pulse at 613.80 nm, where the HCO $\mathrm{X^2A''}$ (0,0,0) $\rightarrow$ $\mathrm{A^2A'}$ (0,9,0) R bandhead[29,30] is located, the HCO absorption was obtained from the photolysis of C3-C7 aldehydes. A pulse/delay generator was used to vary the delay time between the firing of the photolysis and the probe lasers. The photolysis laser pulse energy was measured with a calibrated Joulemeter. Gas pressure was measured at the center of the reaction cell with a capacitance manometer. The absorption cross-section of the aldehyde at each wavelength was determined by monitoring the transmitted photolysis photon intensity as a function of aldehyde pressure in the cell and by applying Beer's law to the experimental data. A fresh aldehyde sample was introduced

Downloaded At: 02:46 30 January 2011

into the cell for each absorption cross-section measurement. In order to obtain reliable determination of the transmitted photolysis fluence as a function of aldehyde pressure in the cell, absorption cross-section measurements typically were carried out over wider aldehyde pressure range than that used for quantum yield measurements. Quantum yield measurements were made at a laser repetition rate of 0.1 Hz to ensure the replenishment of the gas samples between successive laser pulses. The spectrum scan was performed at a laser repetition rate of 1 Hz. All experiments were carried out at a temperature of 293 ± 2 K.

The highest purity propionaldehyde, n-butyraldehyde, n-pentanal, n-hexanal, and n-heptanal were purchased from Aldrich (Milwaukee, WI) and were purified by repeated freeze-pump-thaw cycles at 77 K before each experiment to remove volatile impurities. Formaldehyde was generated by pyrolysis of paraformaldehyde (>95% purity; Aldrich) at 110°C; Fourier transform infrared (FTIR) analysis indicated that formaldehyde thus produced is free of detectable impurities. Nitrogen (>99.999% purity; BOC Gas, Murray Hill, NJ) and chlorine (>99.5% purity; Aldrich) were used without further purification.

Downloaded At: 02:46 30 January 2011

RESULTS AND DISCUSSION

Absorption Cross-Sections of C3-C7 Aldehydes in the 280–330 nm Region

The room-temperature absorption cross-sections of propionaldehyde,[19] n-butyraldehyde,[20] n-pentanal,[21] n-hexanal,[22] and n-heptanal[22] were determined at 5-nm intervals in the 280–330 nm region. They are shown in Fig. 1 and listed in Table 1. These saturated aliphatic aldehydes display a broad absorption band in the near-UV region resulting from an electric dipole-forbidden but vibronically allowed $n \rightarrow *$ transition. The error bars quoted (1σ) express the estimated precision of the cross-section determinations and includes the standard deviation for each measurement (~0.5%) plus the standard deviation about the mean of at least four repeated experimental runs. The overall uncertainty for cross-section measurements, considering both random and systematic errors, is about 5–10% for propionaldehyde at all wavelengths,[19] about 5–10% for n-butyraldehyde in the 280–325 nm region and about 15% at 330 nm,[20] and about 5% for n-pentanal in the 280–325 nm region and about 16% at 330 nm.[21] The room temperature vapor pressures of n-hexanal and n-heptanal are about 8.5 Torr and 2.3 Torr, respectively. The overall uncertainty for n-hexanal cross-section measurements is about 5–10% in the 280–320 nm range and about 16% at 325 and 330 nm.[22] The overall uncertainty for n-heptanal

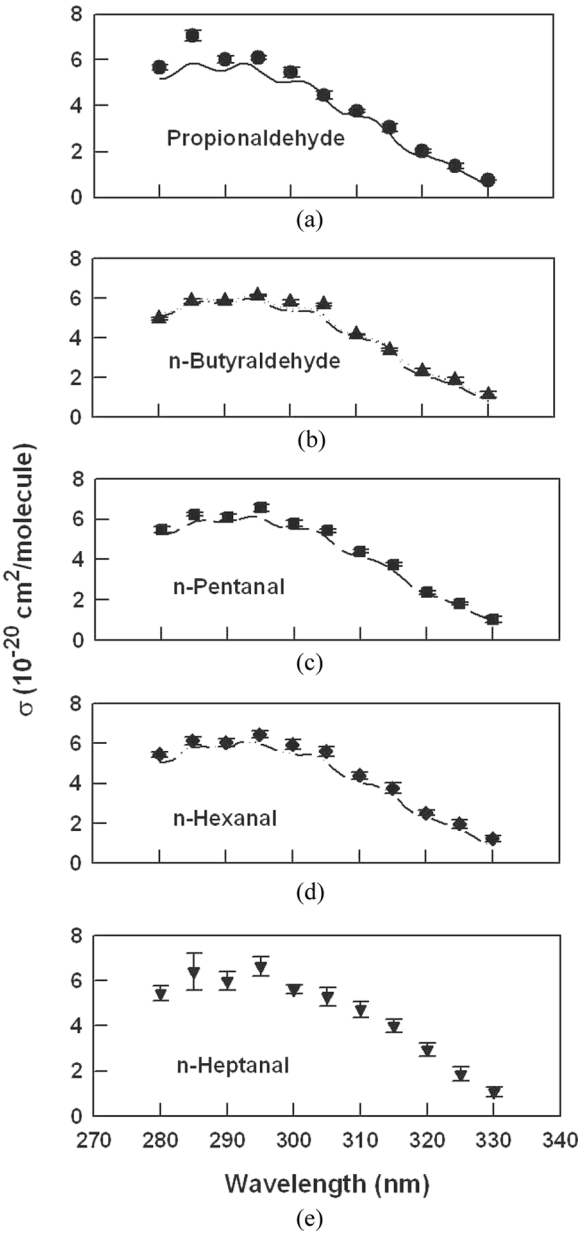

FIGURE 1 **Absorption cross-sections of C3-C7 aldehydes in the 280–330 nm region; (a) propionaldehyde (circles: Chen and Zhu;[19] solid line: Martinez et al.[17]), (b) n-butyraldehyde (triangles: Chen et al.;[20] dotted line: Martinez et al.;[17] dash-dot line: Tadić et al.[31]), (c) n-pentanal (squares: Cronin et al.;[21] medium dash line: Tadić et al.[31]), (d) n-hexanal (diamonds: Tang and Zhu;[22] dash-dot-dot line: Tadić et al.[32]), (e) n-heptanal (inverted triangles: Tang and Zhu[22]).**

TABLE 1 Absorption Cross-Sections (10^{-20} cm^2 Molecule^{-1}, Base e) of C3-C7 Aldehydes versus Wavelength

λ (nm)	σ (prop)[a]	σ (n-butyr)[b]	σ (n-penta)[c]	σ (n-hexan)[d]	σ (n-hepta)[e]
280	5.7 ± 0.1	5.0 ± 0.1	5.5 ± 0.2	5.5 ± 0.1	5.4 ± 0.3
285	7.1 ± 0.2	5.9 ± 0.1	6.2 ± 0.1	6.1 ± 0.2	6.4 ± 0.8
290	6.0 ± 0.2	5.9 ± 0.1	6.1 ± 0.2	6.0 ± 0.2	6.0 ± 0.4
295	6.1 ± 0.1	6.1 ± 0.1	6.6 ± 0.2	6.5 ± 0.2	6.6 ± 0.4
300	5.5 ± 0.2	5.8 ± 0.1	5.8 ± 0.2	5.9 ± 0.3	5.6 ± 0.2
305	4.5 ± 0.2	5.7 ± 0.1	5.4 ± 0.1	5.6 ± 0.2	5.3 ± 0.4
310	3.8 ± 0.1	4.2 ± 0.1	4.4 ± 0.1	4.4 ± 0.2	4.7 ± 0.3
315	3.1 ± 0.2	3.4 ± 0.1	3.7 ± 0.1	3.8 ± 0.3	4.0 ± 0.3
320	2.0 ± 0.1	2.3 ± 0.1	2.4 ± 0.1	2.5 ± 0.1	2.9 ± 0.3
325	1.4 ± 0.1	1.9 ± 0.1	1.8 ± 0.1	2.0 ± 0.2	1.9 ± 0.3
330	0.75 ± 0.01	1.1 ± 0.2	1.0 ± 0.2	1.2 ± 0.2	1.1 ± 0.2

[a]Cross-section data for propionaldehyde were taken from reference 19.
[b]Cross-section data for n-butyraldehyde were taken from reference 20.
[c]Cross-section data for n-pentanal were taken from reference 21.
[d]Cross-section data for n-hexanal were taken from reference 22.
[e]Cross-section data for n-heptanal were taken from reference 22.

Downloaded At: 02:46 30 January 2011

cross-section measurements is below 20% in the 280–320 nm range and below 26% at 325 and 330 nm.[22] The smallest absorption cross-section that can be measured by monitoring the transmitted photolysis fluence as a function of aldehyde pressure in the cell is about 5×10^{-21} cm^2. As seen from Fig. 1, the shape of the near-UV absorption band is similar from propionaldehyde to n-heptanal; the absorption cross-sections in the 295–330 nm region initially increase with chain length from propionaldehyde to n-butyraldehyde, while the cross-section values of n-pentanal, n-hexanal, and n-heptanal are almost the same. Also included in Fig. 1, for comparative purposes, are cross-section results reported by Martinez et al.[17] (propionaldehyde and n-butyraldehyde) and by Tadic et al.[31,32] (n-butyraldehyde, n-pentanal, and n-hexanal). Both the shape of the aldehyde absorption bands and magnitude of the absorption cross sections reported by the various groups are similar, although Martinez et al. and Tadic et al. observed more detailed absorption features due to higher resolution spectra. Except for 285 and 330 nm, cross-section data from this study on propionaldehyde[19] agree to within 10% with those obtained by Martinez et al. The cross-section values in this work for n-butyraldehyde[20] and n-pentanal[21] agree to within 10% with those obtained previously[17,31] in the 280–325 nm region and to within 25% at 330 nm. The cross-section values from this study for n-hexanal[22] agree with Tadic et al.[32] to within 5–10% in the 280–320 nm range, 15% at 325 nm, and 35% at 330 nm.

Time-Resolved Studies of the Photolysis of C3-C7 Aldehydes in the 280–330 nm Region

Shown in Fig. 2 is a cavity ring-down absorption spectrum of the product after 290 nm photolysis of propionaldehyde.[19] The similarity of the product absorption spectrum to the previously reported absorption spectrum[33] of HCO in the same wavelength region indicates that the HCO radical is a photolysis product of propionaldehyde. As seen from Fig. 2, the HCO radical displays a structured absorption band

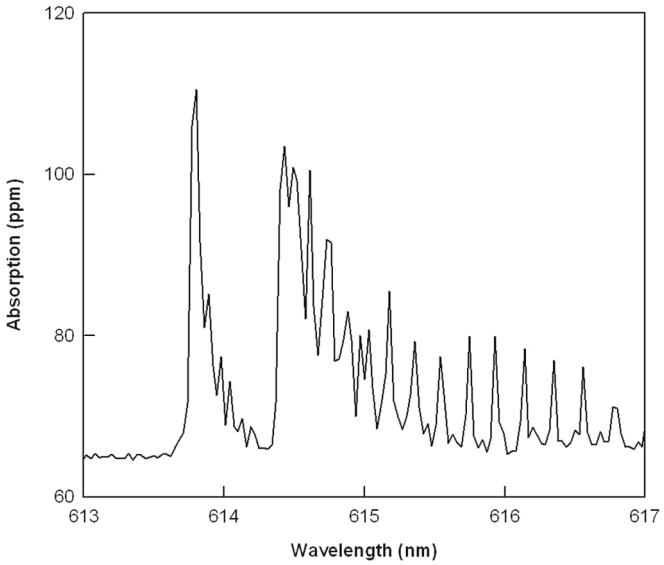

FIGURE 2 Cavity ring-down absorption spectrum of the product[19] after 290 nm photolysis of 5.05 Torr propionaldehyde.

in the 613–617-nm region that can be attributed to individual rotational lines of the $X^2A''(0,0,0) \rightarrow A^2A'$ (0,9,0,) vibrational transition. Similar product absorption spectra were obtained from the photolysis of n-butyraldehyde,[20] n-pentanal,[21] n-hexanal,[22] and n-heptanal.[22] No noticeable difference was observed in the shape or position of individual peaks in the HCO spectrum obtained from the photolysis of different aldehydes. The cavity ring-down spectrometer was tuned to the HCO X^2A'' (0,0,0) $\rightarrow$ A^2A' (0,9,0) R bandhead at 613.8 nm, and the HCO concentration was followed as a function of time. Presented in Fig. 3 is a temporal profile of HCO from the 290 nm photolysis of 3 Torr propionaldehyde[19] along with a fitting of the HCO decay profile using the following kinetic scheme:

$$HCO + HCO \longrightarrow H_2CO + CO, \quad (7)$$

$$HCO + C_2H_5 \longrightarrow \text{products}, \quad (8)$$

$$C_2H_5 + C_2H_5 \longrightarrow C_4H_{10}, \quad (9a)$$

$$\longrightarrow C_2H_4 + C_2H_6, \quad (9b)$$

$$HCO + C_2H_5CHO \longrightarrow \text{products}. \quad (10)$$

This modeling scheme assumes that $HCO + C_2H_5$ is the only important radical formation channel formed from the direct photolysis of propionaldehyde at 290 nm, an assumption supported by the HCO quantum yield of 1.0 ± 0.1 from the photolysis of propionaldehyde at 290 nm described later in this article. Time-resolved HCO decay profiles from the photolysis of 3, 6, and 9 Torr propionaldehyde were compared with profiles calculated by the ACUCHEM simulation program.[34] The following input parameters were used: rate constants for the HCO+HCO, HCO+C_2H_5, C_2H_5+C_2H_5, and HCO+C_2H_5CHO reactions ($k_{HCO+HCO}$, $k_{HCO+C_2H_5}$, $k_{C_2H_5+C_2H_5}$, and $k_{HCO+C_2H_5CHO}$) and the initial HCO concentration ($[HCO]_0$). A literature $k_{C_2H_5+C_2H_5}$ value of 1.9×10^{-11} cm^3 $molecule^{-1}$ s^{-1} was used in the fitting.[35] Initial values of $k_{HCO+HCO}$, $k_{HCO+C_2H_5}$, and $k_{HCO+C_2H_5CHO}$ were provided to the program, and the simulated HCO profiles were compared with the experimental results. After several iterations and adjustments of $k_{HCO+HCO}$, $k_{HCO+C_2H_5}$, and $k_{HCO+C_2H_5CHO}$ values, optimum fittings of the experimental profiles were accomplished. The $k_{HCO+HCO}$, $k_{HCO+C_2H_5}$, and $k_{HCO+C_2H_5CHO}$ values thus extracted[19] are $(6.0 \pm 1.5) \times 10^{-11}$, $(6.5 + 1.5) \times 10^{-11}$, and $(1.5 + 0.2) \times 10^{-14}$ cm^3 $molecule^{-1}s^{-1}$, respectively, where uncertainty (1σ) represents the variation in rate constants required in order for the calculated HCO profiles to fit the measured profiles. The HCO decay profiles at all three propionaldehyde pressures are well-fitted by these extracted $k_{HCO+HCO}$, $k_{HCO+C_2H_5}$, and $k_{HCO+C_2H_5CHO}$ values. The accuracy of the $k_{HCO+HCO}$ and $k_{HCO+C_2H_5}$ measurements is affected by accuracy in the determination of the HCO absorption cross-section (σ_{HCO}) and the HCO's initial concentration ($[HCO]_0$), and by the time resolution of the cavity ring-down spectroscopy ($\sim$17–21 μs around 613 nm). The initial HCO concentration was in the range of 4.8×10^{13} to 8.5×10^{13} cm^{-3} for propionaldehyde pressures between 3 and 9 Torr. The overall uncertainty for the extracted $k_{HCO+HCO}$ and $k_{HCO+C_2H_5}$ is about 50%. Values of $k_{HCO+HCO}$ and $k_{HCO+C_2H_5}$ thus obtained agree well with the recommended rate constant[25] for the HCO+HCO reaction ($k = 2.5 \times 10^{-11}$–10.0×10^{-11} cm^3 $molecule^{-1}$ s^{-1} at 300 K) and the previously reported rate constant[36] for the C_2H_5+HCO reaction ($(7.2 \pm 1.6) \times 10^{-11}$ cm^3 $molecule^{-1}s^{-1}$). The influence of the numerical value of $k_{HCO+C_2H_5CHO}$ on the HCO decay profiles becomes important at time scales on the order of hundreds of microseconds. Because the HCO decay profiles were measured at several propionaldehyde pressures under the condition that $[HCO]0 << [C_2H_5CHO]_0$, the overall uncertainty in the value of $k_{HCO+C_2H_5CHO}$ is about 20%. Inclusion of the

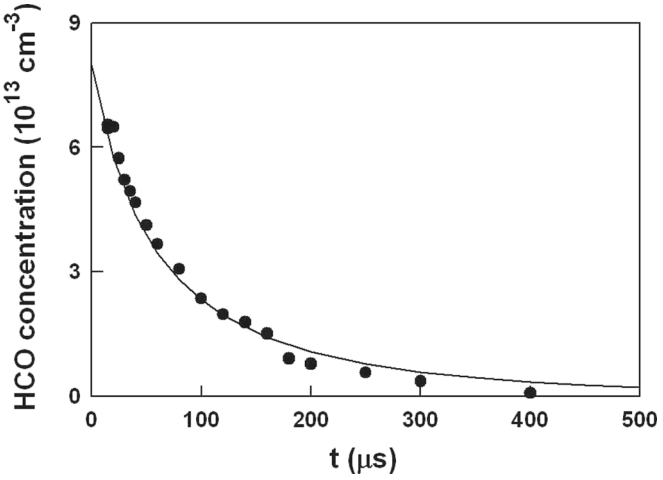

FIGURE 3 **Time profile of the HCO radical from the photolysis of 3 Torr propionaldehyde at 290 nm (adapted from reference 19). Circles represent experimental determinations. Solid line is a simulated profile calculated using the ACUCHEM simulation program.**

Downloaded At: 02:46 30 January 2011

$HCO+C_2H_5CHO$ reaction in the simulation leads to a better fit of HCO decay profiles than is obtained without inclusion of this reaction, especially on the time scale of hundreds of μs. Consistent measurements of the rate constant of the $HCO+C_2H_5CHO$ reaction were obtained. Also, the HCO+HCO, HCO+R, and HCO+RCHO rate constants (R = n-C_4H_9 and n-C_5H_{11}) from the photolysis of n-pentanal[21] and n-hexanal were measured.[22]

HCO Radical Quantum Yields from the Photolysis of C3-C7 Aldehydes in the 280–330 nm Region

The HCO radical quantum yields from the photolysis of propionaldehyde, n-butyraldehyde, n-pentanal, n-hexanal, and n-heptanal were determined from the ratio of the HCO concentration produced in the pump/probe laser overlapping region to the absorbed photon density in the same region. The overlap region can be viewed as a rectangular solid with its center overlapping that of the cell, with width and height defined by those of the photolysis beam, and length of the rectangular solid defined by (beam width) $\times$ $(\tan 15^\circ)^{-1}$, where 15 degrees is the crossing angle between the pump and the probe laser beams. The photolysis beam is absorbed by aldehydes over the entire level arm through which it travels. The absorbed photolysis photon density in the pump/probe laser overlap region can be derived from the difference in the transmitted photolysis beam energy entering (E_{in}) and leaving (E_{out}) that region, the individual photon energy (hc/λ) at the photolysis wavelength (λ), and the volume (v) of the overlapping region by the following equations:

$$\text{Absorbed photon density} = \frac{E_{in} - E_{out}}{h\frac{c}{\lambda}v},$$

$$\begin{aligned} \text{v} &= \text{beam width} \times \text{beam height} \\ &\quad \times \text{length of the rectangular solid} \\ &= \text{beam width} \times \text{ beam height} \\ &\quad \times (\text{beam width}) \times (\tan 15^\circ)^{-1} \end{aligned}$$

The photolysis beam energy entering or leaving the pump/probe laser overlapping region can be calculated from the incident photolysis beam energy entering the cell (E_0), the absorption cross-section (σ) and the density (n) of aldehyde in the cell, and the absorbing path length by application of Beer's law:

$$E_{in} = E_0 \cdot \exp(-\sigma n l_1)$$

$$E_{out} = E_0 \cdot \exp(-\sigma n l_2)$$

where l_1 is the distance between the photolysis beam entry point and the beginning of the pump/probe laser overlap region, and l_2 is the distance between the photolysis beam entry point and the end of the pump/probe laser overlap region. The incident photolysis beam energy was measured by a calibrated Joulemeter (Coherent) placed in front of the cell (pulse energy calibration uncertainty <5%). The incident beam energy inside the cell was corrected for transmission loss at the front cell window and for reflection of the photolysis beam from the rear cell window. The HCO concentration after the photolysis was acquired by measurement of HCO absorption at 613.80 nm at a photolysis and a probe laser delay of 15 µs. To convert HCO absorption into absolute concentration, we determined the absorption cross-section of HCO at the probe laser wavelength either relative to that from the formaldehyde photolysis, $H_2CO+h\nu \rightarrow HCO+H$, for which the recommended HCO quantum yield at each photolysis wavelength is available,[25] or else from the $Cl+H_2CO \rightarrow HCl+HCO$ reaction.[25]

The dependence of the HCO radical quantum yields on C3-C7 aldehyde pressure was examined. Displayed in Figs. 4(a) and 4(b) are plots of the HCO quantum yields (φ_{HCO}) as a function of propionaldehyde pressure at photolysis wavelengths of 290 and 320 nm.[19] The uncorrected HCO radical yields initially decrease with increasing propionaldehyde pressure and then level off at higher aldehyde pressures. This initial decrease of the HCO quantum yield with increasing propionaldehyde pressure possibly results from quenching of the excited precursor to dissociation by the ground-state propionaldehyde molecules, as well as the increasing HCO+HCO, C_2H_5+HCO, and $HCO+C_2H_5CHO$ reactions at higher propionaldehyde pressures. In order to separate the contribution of HCO radical reactions from the quenching process, we have corrected the HCO radical yields for HCO radical reactions at 15 µs; included in Fig. 4 are both the uncorrected

Downloaded At: 02:46 30 January 2011

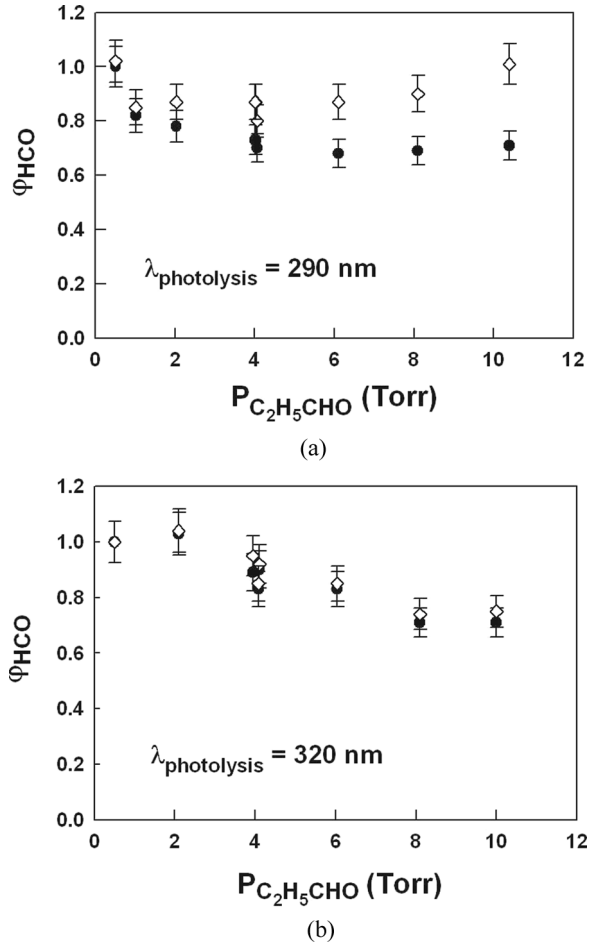

FIGURE 4 **(a) The HCO radical yields as a function of propionaldehyde pressure at photolysis wavelengths of 290 nm (adapted from reference 19). (b) The HCO radical yields as a function of propionaldehyde pressure at the photolysis wavelength of 320 nm (adapted from reference 19). Circles represent uncorrected HCO radical yields. Diamonds represent HCO yields that have been corrected for HCO+HCO, HCO+C_2H_5, and HCO+C_2H_5 CHO reactions at 15 μs.**

and the corrected HCO radical yields. As seen from Fig. 4, there was no propionaldehyde pressure quenching effect when the photolysis study was conducted at 290 nm. The corrected HCO radical yields still decrease with increasing propionaldehyde pressure at 320 nm, suggesting an aldehyde pressure quenching effect at longer photolysis wavelengths. Since 320 nm is close to the photodissociation threshold of propionaldehyde, increasing propionaldehyde pressure may quench the excited state to below the dissociation limit. (In the absence of values for the exact photodissociation threshold of propionaldehyde, and the vibrational density of states of propionaldehyde in the ground and exited electronic states, it is difficult to predict with accuracy the number of collisions needed at each photolysis wavelength to quench the excited state to below the dissociation limit.) The corrected reciprocal HCO quantum yields were plotted against propionaldehyde concentration ([C_2H_5CHO]) according to the Stern–Volmer equation:

$$1/\varphi_{HCO} = 1/\varphi_{HCO^\circ} + (k^Q_{C_2H_5CHO}/k^D_{C_2H_5CHO}) \cdot [C_2H_5CHO] \quad (11)$$

where φ_{HCO}° is the HCO quantum yield extrapolated to zero propionaldehyde pressure, and $k^Q_{C_2H_5CHO}/k^D_{C_2H_5CHO}$ is the ratio of quenching to unimolecular decay rate constant of the excited propionaldehyde. For those photolysis wavelengths at which the corrected HCO yields are independent of propionaldehyde pressure, $k^Q_{C_2H_5CHO}/k^D_{C_2H_5CHO}$ is equal to zero. Illustrated in Fig. 5 is a plot of $1/\varphi_{HCO}$ vs. [C_2H_5CHO] at 320-nm photodissociation wavelength;[19] note that the Stern–Volmer plot is linear, suggesting collisional electronic quenching of excited propionaldehyde. Experimentally derived φ_{HCO}° from the photolysis of propionaldehyde, n-butyraldehyde, n-pentanal, n-hexanal, and n-heptanal as a function of the photolysis wavelength are tabulated in Table 2 and plotted in Fig. 6. As seen from Fig. 6, the zero-pressure HCO quantum yields from the photolysis of propionaldehyde,[19] n-butyraldehyde,[20] n-pentanal,[21] n-hexanal,[22] and n-heptanal[22] exhibit significant wavelength dependencies and decrease at both the longer-wavelength and shorter-wavelength ends. The decrease in HCO quantum yields with decreasing wavelength at the shorter-wavelength end can possibly be attributed to the opening of an additional photolysis pathway, such as the formation of RH+CO, at higher photon energies. The reduced HCO quantum yields at the longer-wavelength end may be the result of dissociation at near-threshold wavelengths. The peak HCO quantum yields from the photolysis of propionaldehyde,[19] n-butyraldehyde,[20] n-pentanal,[21] n-hexanal,[22] and n-heptanal[22] are 1.0 ± 0.1, 0.8 ± 0.1, 0.20 ± 0.06, 0.15 ± 0.02, and 0.15 ± 0.06, respectively, where the uncertainty (1σ) represents experimental scatter. The HCO quantum yield of 1.0 ± 0.1 from propionaldehyde photolysis at 310 nm indicates that $C_2H_5CHO + h\nu \rightarrow C_2H_5 + HCO$ is the dominant photolysis pathway. The difference in the peak HCO quantum yields from propionaldehyde to n-butyraldehyde has been attributed to the opening of the Norrish II channel from the photolysis of n-butyraldehyde. The peak HCO radical yields

Downloaded At: 02:46 30 January 2011

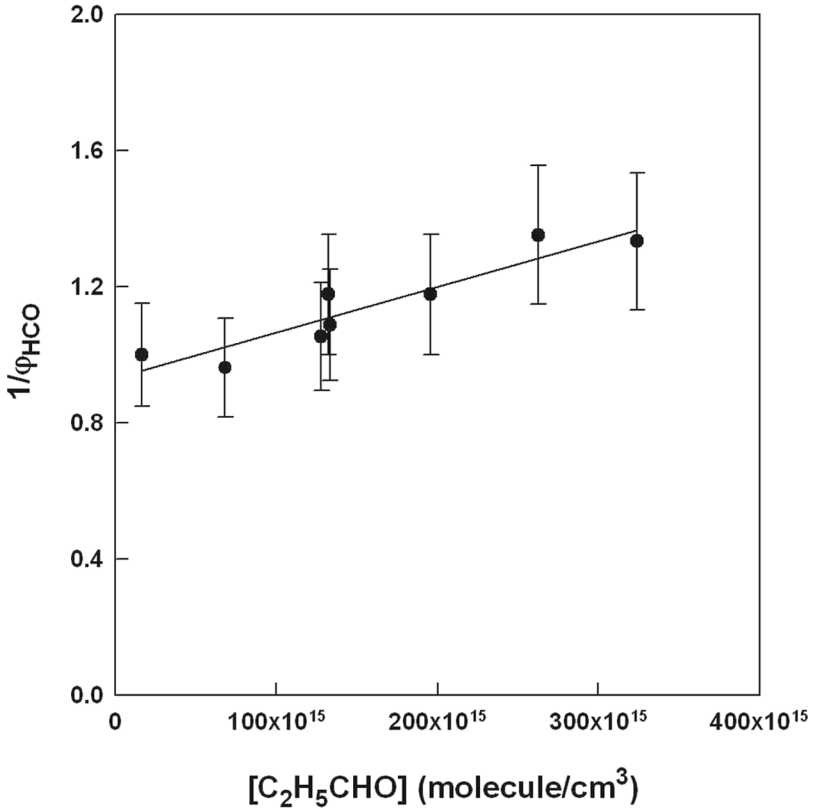

FIGURE 5 **A Stern–Volmer plot of the reciprocal HCO yields from 320 nm photolysis of propionaldehyde (adapted from reference 19). Circles represent experimental data. Solid line is a fit of the experimental data to the Stern–Volmer expression.**

Downloaded At: 02:46 30 January 2011

decrease with increasing alkyl chain length between n-butyraldehyde and n-pentanal, but this trend of decrease does not continue for aldehydes with chain length equal to or longer than five carbon atoms. The shape of the curve relating HCO quantum yield to wavelength, and the magnitude of the HCO radical yields, are similar for n-pentanal, n-hexanal, and n-heptanal. Since n-pentanal, n-hexanal, and n-heptanal have γ-hydrogen atoms or δ-hydrogen atoms that can be readily abstracted intramolecularly by the O atom to form Norrish type II photoelimination products or to form photocyclization products,

TABLE 2 **Values of φ°_{HCO} from the Photolysis of C3-C7 Aldehydes**

λ (nm)	φ°_{HCO} (prop)[a]	φ°_{HCO} (n-butyr)[b]	φ°_{HCO} (n-penta)[c]	φ°_{HCO} (n-hexan)[d]	φ°_{HCO} (n-hepta)[e]
280	0.9 ± 0.1	0.2 ± 0.1	0.06 ± 0.01	0.07 ± 0.01	0.08 ± 0.01
285	1.0 ± 0.1	0.2 ± 0.1	0.10 ± 0.01	0.09 ± 0.02	0.09 ± 0.01
290	1.0 ± 0.1	0.3 ± 0.1	0.10 ± 0.02	0.09 ± 0.01	0.10 ± 0.02
295	1.0 ± 0.1	0.3 ± 0.1	0.14 ± 0.01	0.10 ± 0.01	0.12 ± 0.03
300	0.9 ± 0.1	0.3 ± 0.1	0.10 ± 0.02	0.09 ± 0.01	0.11 ± 0.03
305	1.0 ± 0.1	0.5 ± 0.1	0.15 ± 0.02	0.12 ± 0.01	0.14 ± 0.04
310	1.0 ± 0.1	0.7 ± 0.1	0.14 ± 0.02	0.15 ± 0.02	0.15 ± 0.06
315	0.9 ± 0.1	0.8 ± 0.1	0.20 ± 0.06	0.14 ± 0.02	0.10 ± 0.01
320	1.1 ± 0.1	0.8 ± 0.1	0.14 ± 0.02	0.10 ± 0.01	0.11 ± 0.02
325	1.1 ± 0.1	0.7 ± 0.1	0.09 ± 0.03	0.10 ± 0.02	0.10 ± 0.02
330	0.8 ± 0.1	0.6 ± 0.1	0.09 ± 0.02	0.08 ± 0.02	0.10 ± 0.03

[a]Quantum yield values for propionaldehyde were taken from reference 19.
[b]Quantum yield values for n-butyraldehyde were taken from reference 20.
[c]Quantum yield values for n-pentanal were taken from reference 21.
[d]Quantum yield values for n-hexanal were taken from reference 22.
[e]Quantum yield values for n-heptanal were taken from reference 22.

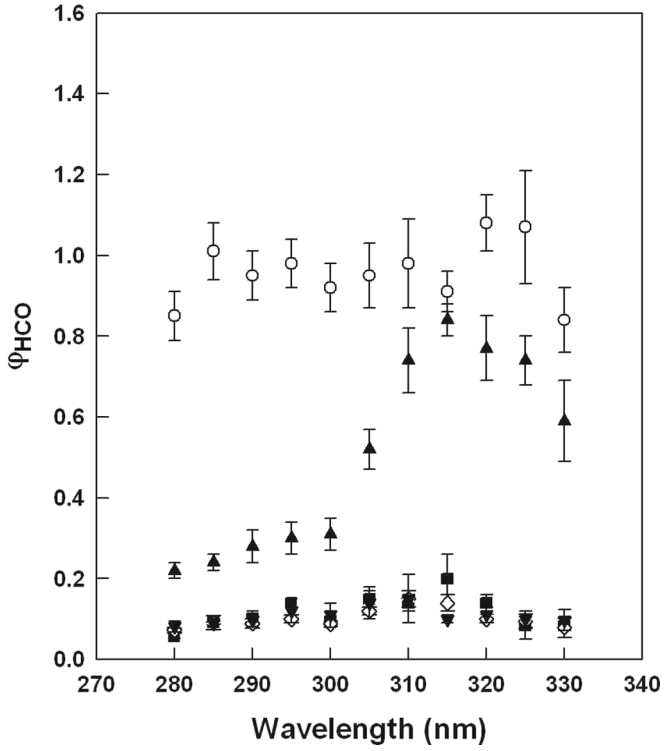

FIGURE 6 **Zero pressure HCO quantum yields from the photolysis of C3-C7 aldehydes as a function of photodissociation wavelength. Circles: propionaldehyde;[19] triangles: n-butyraldehyde,[20] squares: n-pentanal,[21] diamonds: n-hexanal,[22] inverted triangles: n-heptanal.[22]**

Downloaded At: 02:46 30 January 2011

similar yields of intramolecular isomerization products can be expected from the photolysis of each of these longer-chain aldehydes. By extension, similar HCO radical yields can be expected from the photolysis of aldehydes with a chain length of five carbon atoms or longer. On the other hand, n-butyraldehyde only has primary γ-hydrogen atoms, which are less reactive than the secondary γ-hydrogen atoms. Therefore, radical formation is the preferred process from n-butyraldehyde photolysis.

We examined the dependence of the HCO radical quantum yields on total pressure by holding the aldehyde pressure constant while changing the nitrogen buffer-gas pressure. The HCO radical quantum yields were found to be independent of total pressure (6–387 Torr) to within the experimental error limit in the 280–330 nm region. For the purpose of atmospheric modeling, we consider it a good approximation to set the zero-pressure HCO quantum yields from the photolysis of C3-C7 aldehydes equal to those in the presence of 760 Torr of nitrogen, since nitrogen is an extremely poor quencher of vibronically excited aldehyde.

The quantum yields of CO and C_2H_6 from the photodissociation of propionaldehyde in air were measured by Shepson and Heicklen.[37] Those authors obtained quantum yields for the C_2H_5+HCO channel from the difference in quantum yields between CO and C_2H_6; the yields were 0.13, 0.28, 0.22, 0.26, 0.067, and 0.18 at 254, 280, 302, 313, 326, and 334 nm, respectively, in 760 Torr of air. Heicklen et al.[38] acquired C_2H_5 quantum yields either by flash photolysis of propionaldehyde in air and monitoring the UV absorption of total peroxy radicals ($C_2H_5O_2$+HO_2) at 250 nm, or by steady-state photolysis of propionaldehyde in oxygen. Their C_2H_5 yields were 0.89, 0.85, 0.50, 0.26, and 0.15 at 294, 302, 313, 325, and 334 nm, respectively, in 760 Torr air. Our HCO quantum yields from propionaldehyde photolysis[19] are 0.9 ± 0.1, 1.0 ± 0.1, 1.0 ± 0.1, 1.0 ± 0.1, 0.9 ± 0.1, 1.0 ± 0.1, 1.0 ± 0.1, 0.9 ± 0.1, 1.1 ± 0.1, 1.1 ± 0.1, and 0.8 ± 0.1 at 280, 285, 290, 295, 300, 305, 310, 315, 320, 325, and 330 nm, respectively, at 760 Torr nitrogen pressure. The HCO yields from this study are much larger than the C_2H_5 yields reported by Shepson and Heicklen.[37] There is a good agreement between the 295- and 300-nm HCO yields determined by Chen and Zhu[19] and the 294 and 302 nm C_2H_5 yields reported by Heicklen et al.[38] However, these HCO yields at 315 and 325 nm are 1.8–4.2 times the previously reported[38] C_2H_5 yields at 313 and 325 nm. Since both the ground-state oxygen molecule and the first electronically excited state of propionaldehyde are triplet, there might be an electronic-to-electronic energy transfer ($E \rightarrow E$) between excited propionaldehyde and oxygen. This quenching effect would become more pronounced at the longer wavelength tail where dissociation is near threshold. Another plausible explanation for this difference in radical yields in the presence and absence of oxygen is that the complex chemistry involved in the presence of oxygen might introduce greater uncertainties in the results of Heicklen et al.[38]

Förgeteg et al.[39] investigated the photolysis of n-butyraldehyde at 313 nm by analyzing the yields of 20 end-products. They found the primary photolysis pathways to be n-$C_3H_7CHO+h\nu \rightarrow$ n-C_3H_7+HCO ($\varphi = 0.34$) and n-$C_3H_7CHO+h\nu \rightarrow C_2H_4+CH_3CHO$ ($\varphi = 0.17$). The zero pressure HCO quantum yield (0.8) at 313 nm obtained by Chen et al.[20] is 2.4 times the yield obtained by Förgeteg

et al. Since the HCO yield reported by Förgeteg et al. was obtained through end-product measurements and at an n-butyraldehyde pressure of 100 Torr, it is subject to more uncertainties. Tadić et al.[31,32,40] recently characterized photo-oxidation of n-butyraldehyde, n-pentanal, n-hexanal, and n-heptanal in air by combining UV lamp photolysis (275–380 nm) with FTIR. Major products identified include ethene (n-butyraldehyde) or propene (n-pentanal) or 1-butene (n-hexanal) or 1-pentene (n-heptanal), CO, vinylalcohol, and acetaldehyde. They found the total photolysis quantum yields to be slightly dependent on the total pressure. The yield of the radical channel or Norrish II channel was derived from the ratio of the amount of CO or alkene formed to that of aldehyde consumed. Both the HCO+R channel and the CO+RH channel lead to the formation of CO when aldehyde (RCHO) is photolyzed in air. The relative contributions of the HCO+R channel and the CO+RH channel were not reported in the papers by Tadić et al.[31,32,40] As a Result, a direct comparison of this HCO yield to theirs is not possible. A Significant dependence of the aldehyde HCO quantum yield on nitrogen buffer-gas pressure was not observed over the total pressure range of 8–400 Torr.

Photodissociation Rates to Form HCO Radicals in the Atmosphere

The atmospheric radical formation rates (k_{rad}) from the photolysis of C3-C7 aldehydes were calculated using the actinic solar flux ($J(\lambda)$) reported by Demerjian et al.,[41] and the aldehyde absorption cross-sections ($\sigma(\lambda)$) and the HCO radical quantum yields at 760 Torr nitrogen pressure ($\varphi_{HCO}(\lambda)$) determined by our group,[19–22] using the relationship:

$$k_{rad} = \Sigma\sigma(\lambda) \cdot \varphi_{HCO}(\lambda) \cdot J(\lambda)\Delta\lambda. \qquad (12)$$

Radical-formation rates from the photodissociation of C3-C7 aldehydes were estimated as a function of the zenith angle under cloudless conditions at sea level and for best-estimate albedo (5% in the 290–330 nm region[42]). The results[19–22] are shown in Fig. 7. Our estimated HO_x radical-production rates for zenith angles in the 30–60° range are 3.8×10^{-5} to $1.6 \times 10^{-5}\,s^{-1}$ for propionaldehyde,[19] 3.5×10^{-5} to $1.5 \times 10^{-5}\,s^{-1}$ for n-butyraldehyde,[20] 6.7×10^{-6} to $2.7 \times 10^{-6}\,s^{-1}$ for n-pentanal,[21] 5.8×10^{-6} to $2.4 \times 10^{-6}\,s^{-1}$ for n-hexanal,[22] and 5.9×10^{-6} to $2.5 \times 10^{-6}\,s^{-1}$ for n-heptanal.[22] The OH radical production rates from ozone photolysis followed by $O(^1D)/H_2O$ reaction were calculated using gas-phase ozone UV absorption cross-section and $O(^1D)$ channel quantum yield from ozone photolysis reported in reference 25; they are about 6.6×10^{-5} to $1.5 \times 10^{-5}\,s^{-1}$ for zenith angles in the 30–60° range. Photodissociation of aldehydes can be a significant source of HO_x radicals in polluted, VOC-rich atmospheric environments. Assuming a photolysis quantum yield of unity in the actinic UV region for aldehyde, and using the aldehyde absorption cross-sections,[19–22] the corresponding atmospheric photodissociation lifetimes for propionaldehyde,[19] n-butyraldehyde,[20] n-pentanal,[21] n-hexanal,[22] and n-heptanal[22] are on the order of 6.0–17.4, 4.9–13.7, 4.8–13.4, 4.5–12.6, and 4.4–12.3 h for zenith angles in the 0–60° range. Rate constants[3,5,7–11] for OH radical reactions with propionaldehyde, n-butyraldehyde, n-pentanal, n-hexanal, and n-heptanal are on the order of 1.7×10^{-11}, 2.4×10^{-11}, 2.5×10^{-11}, 2.6×10^{-11}, and $3.0 \times 10^{-11}\,cm^3 molecule^{-1}\,s^{-1}$, respectively; these correspond to OH radical

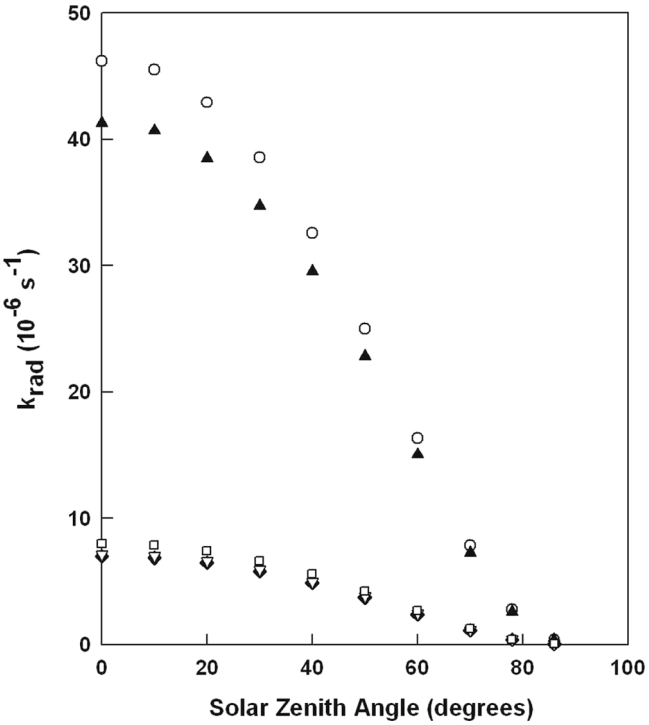

FIGURE 7 **Atmospheric photodissociation rate constants of C3-C7 aldehydes to form radicals as a function of zenith angle at 760 Torr nitrogen pressure. Circles: propionaldehyde,[19] triangles: n-butyraldehyde,[20] squares: n-pentanal,[21] diamonds: n-hexanal,[22] inverted triangles: n-heptanal.[22]**

Downloaded At: 02:46 30 January 2011

reaction lifetimes of 8.2, 5.8, 5.6, 5.3, and 4.6 h for an average noontime OH concentration[40] of $2 \times 10^6\,cm^{-3}$. Therefore, both photolysis and OH radical reactions are important removal pathways for C3-C7 aldehydes in the atmosphere.

Implications for Atmospheric Modeling

In the carbon bond model,[43] aldehydes have been grouped together, while acetaldehyde has been used as a surrogate for aldehydes > C1. Results from our aldehyde photolysis study[20–22] indicate that the photolysis pathways and quantum yields of large aldehydes ($\geq C_4$) are very different from those of acetaldehyde due to the opening of the Norrish II channel and the photocyclization channels for the former. As a result, acetaldehyde photolysis is not representative of the photolysis of large aldehydes. Based upon the results of the photolysis product channel and quantum yield measurements of C3-C7 aldehydes,[19–22] it is recommended that the >C1 aldehydes be divided into three groups in modeling of the photochemistry of saturated aliphatic aldehydes. The first group consists of acetaldehyde and propionaldehyde. The second group consists of n-butyraldehyde. The third group consists of ≥C5 aldehydes. The calculated aldehyde atmospheric photodissociation rates are in the same range as OH radical aldehyde reaction rates.

Downloaded At: 02:46 30 January 2011

ACKNOWLEDGMENTS

We are grateful for the support provided by the National Science Foundation (grants ATM-9610285, ATM-0000252, and ATM-0300294). We thank Dr. Adriana Verschoor for critical readings of the manuscript, and two reviewers for helpful suggestions.

REFERENCES

1. Vairavamurthy, A.; Roberts, J. M.; and Newman, L. Methods for determination of low molecular weight carbonyl compounds in the atmosphere: A review. *Atmospheric Environment* **1992**, *26A*, 1965–1993.
2. Carlier, P.; Hannachi, H.; Mouvier, G. The chemistry of carbonyl compounds in the atmosphere – a review. *Atmospheric Environment* **1986**, *20*, 2079–2099.
3. Semmes, D. H.; Ravishankara, A. R.; Gump-Perkins, C. A.; Wine, P. H. Kinetics of the reactions of hydroxyl radical with aliphatic aldehydes. *International Journal of Chemical Kinetics* **1985**, *17*, 303–313.
4. Dóbé, S.; Khachatryan, L. A.; Bérces, T. Kinetics of reactions of hydroxyl radicals with a series of aliphatic aldehydes. *Berichte der Bunsen Gesellschaft fur Physikalische Chemie-An International Journal of Physical Chemistry* **1989**, *93*, 847–852.
5. Kerr, J. A.; Sheppard, D. W. Kinetics of the reactions of hydroxyl radicals with aldehydes studied under atmospheric conditions. *Environmental Science and Technology* **1981**, *15*, 960–963.
6. Tyndall, G. S.; Staffelbach, T. A.; Orlando, J. J.; Calvert, J. G. Rate coefficients for the reactions of oh radicals with methylglyoxal and acetaldehyde. *International Journal of Chemical Kinetics* **1995**, *27*, 1009–1020.
7. Papagni, C.; Arey, J.; Atkinson, R. Rate constants for the gas-phase reactions of a series of C_3-C_6 aldehydes with OH and NO_3 radicals. *International Journal of Chemical Kinetics* **2000**, *32*, 79–84.
8. Albaladejo, J.; Ballesteros, B.; Jimenez, E.; Martin, P.; Martinez, E. A PLP-LIF kinetic study of the atmospheric reactivity of a series of C_4-C_7 saturated and unsaturated aliphatic aldehydes with OH. *Atmos. Environ.* **2002**, *36*, 3231–3239.
9. Thévenet, R.; Mellouki, A.; LeBras, G. Kinetics of OH and Cl reactions with a series of aldehydes. *Int. J. Chem. Kinet.* **2000**, *32*, 676–685.
10. D'Anna, B.; Andresen, Ø.; Gefen, Z.; Nielsen, C. J. Kinetic study of OH and NO_3 radical reactions with 14 aliphatic aldehydes. *Phys. Chem. Chem. Phy.* **2001**, *3*, 3057–3063.
11. Stemmler, K.; Mengon, W.; Kerr, J. A. Hydroxyl-radical-initiated oxidation of isobutyl isopropyl ether under laboratory conditions related to the troposphere—product studies and proposed mechanism. *J. Chem. Soc. Faraday Trans.* **1997**, *93*, 2865–2875.
12. Finlayson-Pitts, B. J.; Pitts, Jr., J. N. *Atmospheric Chemistry*; John Wiley & Sons, Inc.: New York, 1986.
13. Moortgat, G. K.; Seiler, W.; Warneck, P. Photodissociation of HCHO in air: CO and H_2 quantum yields at 220 and 300 K. *J. Chem. Phys.* **1983**, *78*, 1185–1190.
14. Carmely, Y.; Horowitz, A. The effect of temperature on formaldehyde photooxidation in oxygen-lean atmospheres. *Int. J. Chem. Kinet.* **1984**, *16*, 1585–1598.
15. Ho, P.; Bamford, D. J.; Buss, R. J.; Lee, Y. T.; Moore, C. B. Photodissociation of formaldehyde in a molecular beam. *J. Chem. Phys.* **1982**, *76*, 3630–3636.
16. Horowitz, A.; Calvert, J. G. Wavelength dependence of the primary processes in acetaldehyde photolysis. *J. Phys. Chem.* **1982**, *86*, 3105–3114.
17. Martinez, R. D.; Buitrago, A. A.; Howell, N. W.; Hearn, C. H.; Joens, J. A. The near U.V. absorption spectra of several aliphatic aldehydes and ketones at 300 K. *Atmos. Environ.* **1992**, *26A*, 785–792.
18. Calvert, J. G.; Pitts, Jr., J. N. *Photochemistry*; Wiley: New York, 1966.
19. Chen, Y.; Zhu, L. The wavelength dependence of the photodissociation of propionaldehyde in the 280–330 nm region. *J. Phys. Chem. A* **2001**, *105*, 9689–9696.
20. Chen, Y.; Zhu, L.; Francisco, J. S. Wavelength-dependent photolysis of n-butyraldehyde and i-butyraldehyde in the 280–330 nm region. *J. Phys. Chem. A* **2002**, *106*, 7755–7763.
21. Cronin, T. J.; Zhu, L. Dye laser photolysis of n-pentanal from 280 to 330 nm. *J. Phys. Chem. A* **1998**, *102*, 10274–10279.
22. Tang, Y.; Zhu, L. Wavelength-dependent photolysis of n-hexanal and n-heptanal in the 280–330 nm region. *J. Phys. Chem. A* **2004**, *108*, 8307–8316.
23. O'Keefe, A.; Deacon, D. A. G. Cavity ring-down optical spectrometer for absorption measurements using pulsed laser sources. *Rev. Sci. Instrum.* **1988**, *59*, 2544–2551.
24. O'Keefe, A.; Scherer, J. J.; Cooksy, A. L.; Sheeks, R.; Heath, J.; Saykally, R. J. Cavity ring down dye laser spectroscopy of jet-cooled metal clusters: Cu_2 and Cu_3. *Chem. Phys. Lett.* **1990**, *172*, 214–218.
25. Atkinson, R.; Baulch, D. L.; Cox, R. A.; Hampson, Jr., R. F.; Kerr, J. A.; Troe, J. Evaluated kinetic and photochemical data for atmospheric chemistry. Supplement IV. IUPAC subcommittee on gas kinetic data evaluation for atmospheric chemistry. *J. Phys. Chem. Ref. Data* **1992**, *21*, 1125–1600.
26. Zhu, L.; Cronin, T.; Narang, A. Wavelength-dependent photolysis of i-pentanal and t-pentanal from 280 to 330 nm. *J. Phys. Chem. A* **1999**, *103*, 7248–7253.

27. Zhu, L.; Johnston, G. Kinetics and products of the reaction of the vinoxy radical with O_2. *J. Phys. Chem.* **1995**, *99*, 15114–15119.
28. Zhu, L.; Kellis, D.; Ding, C. F. Photolysis of glyoxal at 193, 248, 308, and 351 nm. *Chem. Phys. Lett.* **1996**, *257*, 487–491.
29. Herzberg, G.; Ramsay, D. A. The 7500 to 4500 Å absorption system of the free HCO radical. *Proc. Royal Soc. (London)* **1955**, *A233*, 34–54.
30. Johns, J. W. C.; Priddle, S. H.; Ramsay, D. A. Electronic absorption spectra of HCO and DCO radicals. *Disc. Faraday Soc.* **1963**, *35*, 90–104.
31. Tadić, J.; Juranic, I.; Moortgat, G. K. Pressure dependence of the photooxidation of selected carbonyl compounds in air: n-Butanal and n-pentanal. *J. Photochem. Photobiol. A Chem.* **2001**, *143*, 169–179.
32. Tadić, J.; Juranic, I.; Moortgat, G. K. Photooxidation of n-hexanal in air. *Molecules* **2001**, *6*, 287–299.
33. Stoeckel, F.; Schuh, M. D.; Goldstein, N.; Atkinson, G. H. Time-resolved intracavity laser spectroscopy: 266 nm photodissociation of acetaldehyde vapor to form HCO. *Chem. Phys.* **1985**, *95*, 135–144.
34. Braun, W.; Herron, J. T. *ACUCHEM/ACUPLOT Computer Program for Modeling Complex Reaction Systems*; National Bureau of Standards: Gaithersburg, MD, 1986.
35. Baulch, D. L.; Cobos, C. J.; Cox, R. A.; Esser, C.; Frank, P.; Just, T.; Kerr, J. A.; Pilling, M. J.; Troe, J.; Walker, R. W.; Warnatz, J. Evaluated kinetic data for combustion modeling. *J. Phys. Chem. Ref. Data* **1992**, *21*, 411–734.
36. Baggott, J. E.; Frey, H. M.; Lightfoot, P. D.; Walsh, R. Reactions of the formyl radical with alkyl radicals. *J. Phys. Chem.* **1987**, *91*, 3386–3393.
37. Shepson, P. B.; Heicklen, J. The wavelength and pressure dependence of the photolysis of propionaldehyde in air. *J. Photochem.* **1982**, *19*, 215–227.
38. Heicklen, J.; Desai, J.; Bahta, A.; Harper, C.; Simonaitis, R. The temperature and wavelength dependence of the photo-oxidation of propionaldehyde. *J. Photochem.* **1986**, *34*, 117–135.
39. Förgeteg, S.; Bérces, T.; Dóbé, S. The kinetics and mechanism of n-butyraldehyde photolysis in the vapor phase at 313 nm. *Int. J. Chem. Kinet.* **1979**, *11*, 219–237.
40. Tadić, J. M.; Juranić, I. O.; Moortgat, G. K. Photooxidation of n-heptanal in air: Norrish type I and II processes and quantum yield total pressure dependency. *J. Chem. Soc. Perkin Trans. II* **2002**, *1*, 135–140.
41. Demerjian, K. L.; Schere, K. L.; Peterson, J. T. Theoretical estimates of actinic (spherically integrated) flux and photolytic rate constants of atmospheric species in the lower troposphere. *Adv. Environ. Sci. Technol.* **1980**, *10*, 369–441.
42. Coulson, K. L.; Reynolds, D. W. The spectral reflectance of natural surfaces. *J. App. Meteorol.* **1971**, *10*, 1285–1295.
43. Gery, M. W.; Whitten, G. Z.; Killus, J. P.; Dodge, M. C. A photochemical kinetics mechanism for urban and regional scale computer modeling. *J. Geophys. Res.* **1989**, *94*, 12925–12956.

Downloaded At: 02:46 30 January 2011